Geophysics of Chemical Heterogeneity in the Mantle

Lars Stixrude and Carolina Lithgow-Bertelloni

Department of Earth Sciences, University College London, WC1E 6BT London, United Kingdom; email: l.stixrude@ucl.ac.uk, c.lithgow-bertelloni@ucl.ac.uk

Annu. Rev. Earth Planet. Sci. 2012. 40:569–95

First published online as a Review in Advance on March 8, 2012

The *Annual Review of Earth and Planetary Sciences* is online at earth.annualreviews.org

This article's doi: 10.1146/annurev.earth.36.031207.124244

0084-6597/12/0530-0569$20.00

Keywords

plate tectonics, phase equilibria, elasticity, lower mantle, transition zone

Abstract

Chemical heterogeneity, produced by the near-surface rock cycle and dominated volumetrically by subducted oceanic crust and its depleted residue, is continuously subducted into the mantle. This lithologic-scale chemical heterogeneity may survive in the mantle for as long as the age of Earth because chemical diffusion is inefficient. Estimates of rates of subduction and mantle processing over geologic history indicate that most or all of the mantle may be composed of lithologically heterogeneous material. Mineralogical models of the mantle show that chemical heterogeneity over many decades in length scale may be detectable by geophysical probes via its influence on seismic-wave propagation. Grain-scale heterogeneity influences the aggregate absolute seismic velocity and its lateral variation with temperature. The elastic-wave velocity contrast associated with lithologic-scale heterogeneity may be sufficient to produce observable scattering of short-period seismic waves.

MANTLE HETEROGENEITY, THE ROCK CYCLE, AND PLATE TECTONICS

The rock cycle is a heterogeneity-producing engine that serves as the cornerstone of geology: Without lithologic heterogeneity, geologic maps would not be very informative. Igneous processes produce, transport, and collect partial melt and leave behind a residue, both of which differ in composition from the source material. Igneous processes act like a Maxwell demon, constantly sorting more-siliceous from less-siliceous material. In this way, the basis of much of our understanding of Earth's history rests on the thermodynamics of incongruent melting to which multicomponent systems, such as Earth's mantle, are subject. Sedimentary processes can act to further segregate and enrich material via transport and reaction with the hydrosphere and atmosphere, for example, by the accumulation of ores or carbonate platforms.

The rock cycle emphasizes how the production of heterogeneity relies on the presence of boundary layers. The formation of igneous rocks from magma relies on the presence of a thermal boundary layer in which the temperature decreases rapidly below the solidus with increasing height, preserving melts in frozen form. The upper thermal boundary layer facilitates subduction, via thermal contraction, and the return of heterogeneity to the deep mantle. The accumulation of magma at the surface depends on the presence of the large density contrast with the overlying ocean and atmosphere. Density contrasts among air, water, and rock drive the transport and accumulation of terrigenous sediment. The chemical boundary layer at the surface (between solid and fluid spheres) is where the generation of sedimentary material is localized.

The mantle below the surface boundary layer is the source of energy for and an active participant in the rock cycle. Heterogeneity produced near the surface is constantly being added via subduction back into the mantle. Some of this subducted material continues its journey around the shallow rock cycle by returning to the surface in arc magmas (Plank & Langmuir 1998). But the great majority of the subducted mass, in the form of the oceanic crust and its depleted residue, continues its descent to much greater depths. From tomographic imaging and comparisons with the history of past subduction, we now have considerable evidence that at least some subducting slabs traverse the entire mantle, whereas others may stagnate, at least temporarily, in the transition zone (Fukao et al. 2009, Grand et al. 1997, Lithgow-Bertelloni & Richards 1998).

Once heterogeneity is produced, it is difficult to destroy. Dating of rocks demonstrates that lithologic contrasts can survive for billions of years. The rate of chemical diffusion increases exponentially with temperature, but even in the mantle, it is sufficiently slow that subducted heterogeneity can last billions of years (Hofmann & Hart 1978, Holzapfel et al. 2005). Thus, whereas the seismic signature of subducting slabs becomes more difficult to detect once they reach the core-mantle boundary (Ricard et al. 2005), a journey that takes 100–200 million years (Ma) (Lithgow-Bertelloni & Richards 1998, van der Meer et al. 2010), the chemical heterogeneity that they carry is likely to survive for much longer. The slab material will be swept into the overlying convective flow and remain lithologically heterogeneous until it is thinned to such an extent that chemical diffusion becomes effective (Allegre & Turcotte 1986, Kellogg & Turcotte 1990). One thus expects not only current subduction, but the entire history of subduction, for which there is at least some evidence back to 3 billion years (Ga) (Chen et al. 2009, Nutman 2006, Shirey & Richardson 2011), to contribute to mantle heterogeneity. In this way, the mantle, because of its large mass, acts as a time capsule of geological heterogeneity, preserving it for much longer than it can survive on the ocean floor (<200 Ma) or on much of the continents (average age 2 Ga) (Taylor & Mclennan 1995). Indeed, it is likely that subducted oceanic crust and its complementary residue retain their lithologic integrity until they are sampled again by the mid-ocean ridge melting process. A variety of analyses indicate that the entire mantle has been

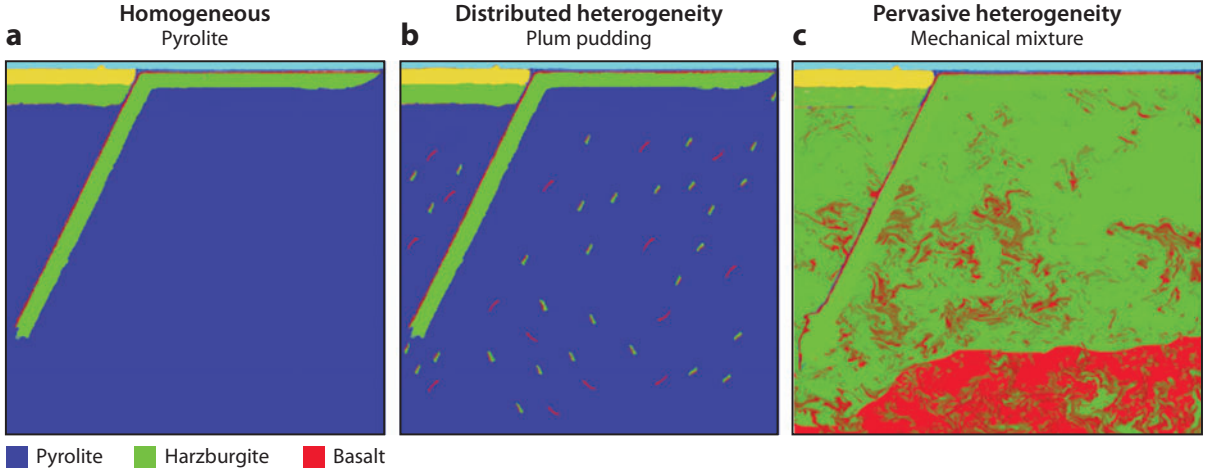

Figure 1

Models of chemical heterogeneity in the mantle. (*a*) Model represents the conventional view that much of the mantle is homogeneous and equal in composition to a fertile peridotite (pyrolite) that produces MORB on partial melting. This model requires that the heterogeneity in the subducted slab be rapidly destroyed by chemical diffusion. (*b*) Model admits survival of small amounts of subducted heterogeneity (plums) within a largely pyrolitic mantle. (*c*) Model of pervasive heterogeneity follows from three assumptions: (*i*) that the entire mantle has been processed through the mid-ocean ridge, (*ii*) that chemical diffusion is sufficiently slow that no heterogeneity has been destroyed, and (*iii*) that subduction has been operative for most of Earth's history. Accumulation of basalt at the base results if it is denser than peridotite in the lower mantle.

processed approximately once over the age of Earth so that some fraction of subducted crust likely remains from the beginning of plate tectonics (Allegre & Turcotte 1986, Davies 2009b, Korenaga 2008).

At the mantle's base, the magnitude of the thermal and chemical boundary layers exceeds those at the surface: The density contrast between mantle and core is larger than that between crust and atmosphere, and the temperature contrast, though still poorly constrained, may exceed 1300 K (Jeanloz & Morris 1986, Knittle & Jeanloz 1991, Nimmo et al. 2004, Steinle-Neumann et al. 2002). The density contrast at the base of the mantle may serve, similar to the surface boundary, to accumulate heterogeneity. If subducted oceanic crust is denser than depleted residue at depth, and the basal temperature is high enough to allow the crust to delaminate, it may accumulate at the base of the mantle (Christensen & Hofmann 1994).

These fundamental considerations lead us to reconsider cartoons that have been used to represent chemical heterogeneity in the mantle (**Figure 1**). At one end of the conceptual spectrum (**Figure 1*a***), we may place the pyrolite model and its descendants (Green & Ringwood 1967). This model views the MORB source or much larger portions of the mantle as being chemically homogeneous and similar in composition to a fertile peridotite, such as a garnet lherzolite. The pyrolite model has had considerable success in explaining the composition of mid-ocean ridge basalts, and the relationship between lava chemistry, crustal thickness, mantle temperature, and ridge height (Klein & Langmuir 1987, McKenzie & Bickle 1988, Workman & Hart 2005). The pyrolite model has served as the starting point for models of whole-mantle structure (Cammarano et al. 2005, Matas et al. 2007, Stixrude et al. 1992, Weidner 1985). And yet, the pyrolite model of the mantle cannot be physically correct. For the mantle to be homogeneous requires subducted heterogeneity to be destroyed on an unrealistically short timescale: one mantle overturn time (~100–200 Ma). An intermediate model has been suggested by a number of studies (**Figure 1*b***)

in which the pyrolite is modified by the addition of enriched and depleted blobs (Davies 1984, Helffrich & Wood 2001, Ito & Mahoney 2005).

At the opposite end of the conceptual spectrum, we may consider a mantle that is completely processed and heterogeneous on all scales (**Figure 1*c***). In this case, subducted heterogeneity is preserved over the age of Earth, or at least over the residence time of oceanic crust in the mantle, so that the mantle is continuously filled with heterogeneous material. Length scales of oceanic crustal heterogeneity range from that of recently subducted crust (∼7 km) to ancient subducted material that has been convectively thinned by a factor of 10^6 (i.e., down to the chemical diffusion length scale of 1 cm), and material that has accumulated into large piles ∼1000 km across. In this end-member view, the entire mantle has been processed and no material point of the mantle is equal in composition to pyrolite.

The great majority of lithologic chemical heterogeneity in the mantle is likely to derive from subducted oceanic crust and its depleted residue, which accounts for more than 90% of all volcanic production on Earth and which is efficiently subducted (Parsons 1982, Reymer & Schubert 1984, White et al. 1992). We focus on this source of chemical heterogeneity because of its volumetric significance and because oceanic crustal chemistry and subduction rates are well constrained over the Cenozoic (Becker et al. 2009) and can at least be estimated over most of Earth's history from continental paleomagnetism (Ulrich & van der Voo 1981). Other sources of mantle chemical heterogeneity exist, although their relative contribution to mantle heterogeneity is either smaller or less certain. Some fraction of continent-derived and carbonate sedimentary material is likely subducted beyond the magma genetic zone (Loubet et al. 1988, Weaver 1991, Ye et al. 2000). The core-mantle boundary layer may be the source of additional chemical heterogeneity via reaction between mantle and core (Knittle & Jeanloz 1991, Takafuji et al. 2005). Indeed, there is some evidence from isotope geochemistry that such reactions take place (Brandon & Walker 2005). It has also been suggested that non–mid-ocean ridge silicate melting processes may contribute substantially to mantle chemical heterogeneity. For example, melting processes in the early Earth may have led to deep melt segregation that has survived for long periods of time (Boyet & Carlson 2005, Labrosse et al. 2007, Lee et al. 2010).

Detection of chemical heterogeneity by geophysical means is challenging for a number of reasons and makes it difficult to decide among the models of **Figure 1** on the basis of direct probes of the deep Earth alone. The first difficulty is that spatial resolution is limited in the deep Earth. The best achievable spatial resolution can be related to the wavelength of the probe, approximately 10 km for a P-wave or 100 km for an S-wave, at typical frequencies of 1 Hz and 50 mHz, respectively, and velocities typical of the lower mantle. Tomographic models typically have spatial resolution that is much coarser than the seismic wavelength, perhaps 200 km in the radial direction (Ritsema et al. 2007). This is sufficient to image large chemically distinct piles, but not a parcel of recently subducted oceanic crust. Greater spatial resolution is obtained by examining individual seismograms from slightly different paths, and small features that are comparable in size to the seismic wavelength are detectable via reflection and scattering (Hedlin et al. 1997, Kaneshima & Helffrich 2010, Ni et al. 2002).

The second difficulty is that geophysical probes do not measure chemical composition. Instead they are sensitive to a set of physical properties that depend on multiple factors. For example, in the case of seismic-wave velocities, we must disentangle at least three sources of heterogeneity, all of which have comparable magnitudes, due to variations in physical properties with chemical composition, temperature, and phase. For example, the subducting slab is colder than surrounding mantle on its descent, accounting for much of its seismic signature in terms of anomalously high seismic-wave velocities (Ricard et al. 2005). Phase transformations also contribute to lateral heterogeneity: The slab undergoes phase transformations as it descends, and these transformations

occur at different pressures than in the surrounding mantle because phase transformations have finite Clapeyron slopes (Anderson 1987). Chemical composition contributes to lateral heterogeneity as well: Subducted basalt and depleted peridotite have distinct physical properties at the same pressure and temperature (Irifune & Ringwood 1993).

The physical properties sensed by geophysical probes are ultimately determined by the atomic-scale structure and bonding of the materials through which the probe passes. Such considerations remind us that chemical heterogeneity in the mantle extends from the subplanetary scale all the way down to that of the grain and the atomic lattice. Atomic-scale heterogeneity is important for understanding the origins of physical properties and also for the relationship of properties measured experimentally to those measured geophysically (Stixrude & Jeanloz 2007). Grain-scale heterogeneity is much larger than lithologic heterogeneity in terms of the contrast in physical properties (Duffy & Anderson 1989). Heterogeneity at this scale manifests itself geophysically in phase transformations. The length scale of lithologic heterogeneity is diminished by convective stirring and chemical diffusion, and it is increased by accumulation to subplanetary scales (Kellogg & Turcotte 1990, Nakagawa et al. 2010).

LENGTH SCALES OF HETEROGENEITY

Atomic Scale

Heterogeneity at the atomic scale underlies our ability to predict and to measure the material properties that govern elastic-wave propagation in Earth. For example, the charge density—the number of electrons per unit volume—varies by two orders of magnitude from on top of the nucleus to the interstitial region between atoms in a typical oxide (Spackman et al. 1987). The charge density is the central quantity in density functional theory, our most powerful means of predicting the properties of deep-Earth materials ab initio (Bukowinski 1994, Kohn 1999). The Kohn-Sham theorem states that there is a unique relationship between the charge density and the total energy (Kohn & Sham 1965). Perturbing the shape of the lattice or the locations of the nuclei allows one to determine the equation of state, the elastic constants, phase transformations, and many other properties (Oganov et al. 2002, Stixrude et al. 1998). Charge-density heterogeneity produces a grating that scatters light with wavelength comparable to the interatomic spacing. This is the basis of X-ray diffraction, which is the most widely used experimental method for determining the density of Earth materials (Fei & Wang 2000).

In the limit of ideal crystals and small deformations, the elasticity of solids is most usefully viewed in the context of the vibrational modes of the crystal lattice (Born & Huang 1954). The theory of the dynamics of perfect crystals is our most powerful way of envisioning the way elastic properties are characterized over a broad range of length scales (Stixrude & Jeanloz 2007). It gives us a formally exact means of relating the elastic-wave velocity of samples ranging in size from the unit cell to, in principle, infinite size, limited only by considerations of surface effects at small scales and of self-gravitation as we approach planetary size (see sidebar, Scaling from Unit Cell to Planet). The material can be treated as a continuum at large scales, and its properties can be derived from consideration of the forces acting between atoms, that is, from a description at the smallest of scales. The seismic-wave velocity of a perfect crystal is determined by its crystal structure and the interatomic forces, and an understanding of dispersion at the atomic scale where the crystal lattice acts as a low-pass filter.

All mantle phases are solid solutions and, thus, contain chemical heterogeneity on the atomic scale. The interaction between solution constituents in nonideal phases can lead to nanometer-scale chemical heterogeneity. Nonideality can lead to inhomogeneous (nonrandom)

SCALING FROM UNIT CELL TO PLANET

A good illustration of length scaling is provided by the normal modes of vibration of a linear chain of identical atoms of mass m separated by a distance a and connected with Hookean springs (bonds) with force constant K. Traveling wave solutions yield the dispersion relation $\omega = 2\sqrt{K/m}\,|\sin(ka/2)|$, where ω is the frequency and $k = 2\pi/\lambda$ is the wavenumber that specifies the wavelength λ of the normal mode of vibration. The group velocity $V_G = \partial\omega/\partial k$ is dispersive (wavelength dependent) such that the crystal lattice is a low-pass filter: Longer waves travel faster than shorter waves. At long wavelength, as $k \to 0$, dispersion vanishes, and group and phase velocities are the same $V = a\sqrt{K/m} = \sqrt{M/\rho}$, where the last equality emphasizes the relationship with the seismic-wave velocity expressed in terms of a longitudinal elastic modulus $M = K/a$ and a density $\rho = m/a^3$. The dispersion due to the crystal lattice is negligible in the usual geophysical context. For ideal crystals, the scaling from laboratory samples to geophysical length scales is essentially exact: Even for millimeter-sized grains the dispersion is only one part in 3000. The presence of defects in real crystals, which leads to anelasticity, modifies this unity of length scales in between those of experiments (MHz-THz) and seismology (Hz-mHz).

arrangement of solution atoms that can significantly influence phase stability and lead to exsolution (Ganguly 2001). The tendency of large atoms to concentrate on grain boundaries may be considered an extreme example of atomic-scale heterogeneity, which may have important implications for understanding the trace-element signature of mantle heterogeneity (Hiraga et al. 2004).

Observations of subgrain-scale chemical heterogeneity in natural systems are ubiquitous and potentially important for understanding larger-scale heterogeneity in the mantle. For example, crystals growing from a magma show compositional zonation reflecting the evolving magma composition (Davidson et al. 2007). Zonation should occur on partial melting as well. Subgrain-scale heterogeneity may develop via chemical diffusion in response to chemical potential gradients, such as exist during reaction between two phases, or forming of one phase from another. For example, during partial melting, incompatible elements must diffuse out of residual crystals, leaving chemical zonation. Chemical diffusion can thus act to increase as well as decrease the length scale of heterogeneity: Diffusion from crystals into the newly formed melt phase increases the scale length of heterogeneity from the spacing between incompatible elements in the crystal to the length scale of the (potentially macroscopic) melt phase.

Grain Scale

The mantle is a multicomponent system for which equilibrium thermodynamics and the phase rule demand the coexistence of multiple phases of different composition and structure. For example, throughout much of the upper mantle, the phases olivine, orthopyroxene, clinopyroxene, and garnet coexist, each of which has distinctive physical properties. Changes in pressure, temperature, or bulk composition alter the compositions and relative proportions of coexisting phases or lead to the appearance of new phases, which can substantially alter the seismic structure of the assemblage.

The contrast in physical properties among coexisting phases is large and reaches 30% in shear-wave velocity in the lower mantle (**Figure 2**). These differences exceed the typical variation of seismic-wave velocities over the mineral stability fields in the upper mantle and transition zone. The velocities of each phase vary with pressure and equilibrium composition in response to partitioning of components among phases. So, for example, the velocity of garnet varies nonmonotonically with depth because of changes in composition. Garnet is the seismically fastest mineral in the upper mantle but the slowest in the transition zone and lower mantle. The fastest mantle

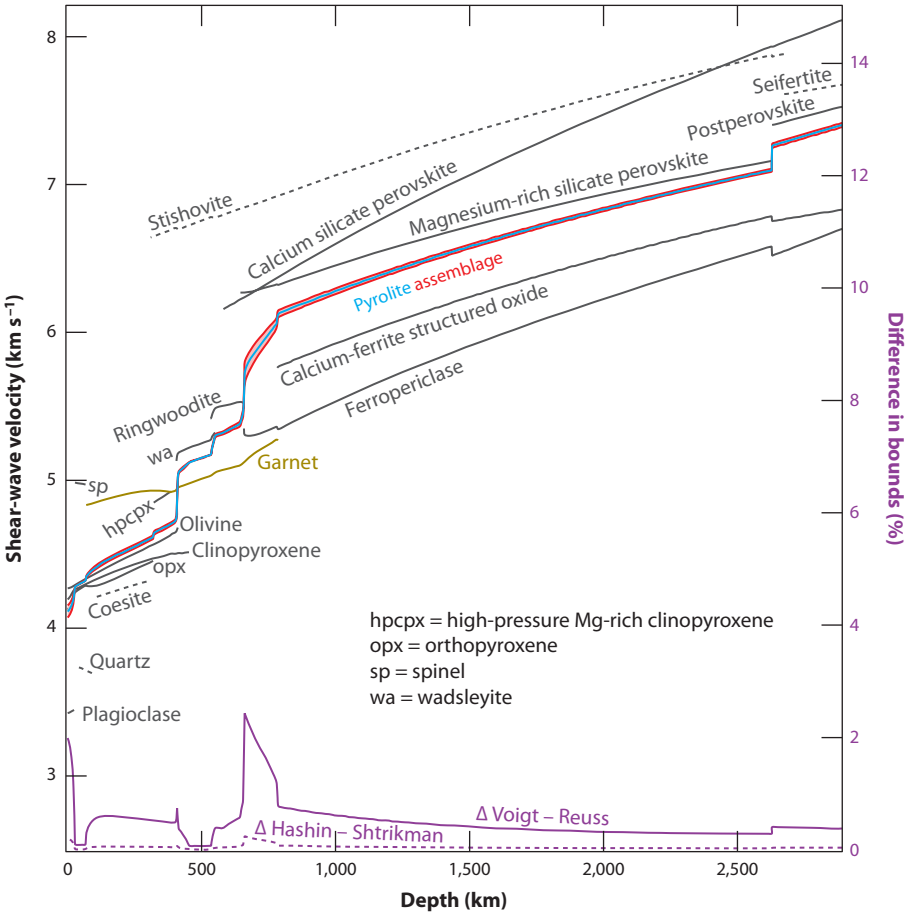

Figure 2

Velocities of mantle phases (*gray lines*), a pyrolite assemblage (*blue with red envelope indicating Voigt-Reuss bounds*), and the difference between Voigt-Reuss bounds (*solid purple line*) and Hashin-Shtrikman bounds (*dashed purple line*) (Hashin & Shtrikman 1963) on the velocity of the assemblage (*purple*, *right-hand axis*) along a self-consistently computed 1600-K isentrope. The velocity of phases is plotted over their pressure range of stability. Silica phases are not stable in pyrolite and are shown for comparison. Computed with HeFESTo (Stixrude & Lithgow-Bertelloni 2011).

phase in these regions is stishovite, except near the base of the mantle where calcium-rich silicate perovskite becomes faster.

How do seismic waves propagate through such a heterogeneous assemblage and at what speed? Because the seismic wavelength is much greater than the size of grains, seismic waves see an averaged structure, and their velocity depends on the details of the arrangement of grains of different velocity. It is possible to place rigorous bounds on the aggregate velocity: The Voigt and Reuss bounds correspond to the assumption of uniform stress and strain throughout the aggregate, respectively (Watt et al. 1976),

$$M_R^* = \left(\sum_\alpha \frac{\phi^\alpha}{M^\alpha} \right)^{-1} < M^* < \sum_\alpha \phi^\alpha M^\alpha = M_V^*, \quad (1)$$

where the sums are over coexisting phases α with volume fractions ϕ^α; M^* is the effective elastic modulus (either the bulk modulus K or the shear modulus G); and M_R^* and M_V^* are the Reuss and Voigt bounds, respectively.

The Voigt and Reuss bounds are physically realized in plane layering in which layers of fast and slow material alternate (Backus 1962). The Voigt and Reuss bounds are narrow throughout most of the mantle, reaching a maximum of 2.5% in the shallow lower mantle and not exceeding 1% elsewhere except near the surface. The Voigt and Reuss bounds place limits on the maximum amount of shape-preferred anisotropy in subsolidus mantle to values that are small compared with that expected from lattice-preferred orientation (Karki et al. 2001). Shape-preferred orientation is not likely to be the dominant source of anisotropy in the subsolidus mantle.

Grain-scale heterogeneity manifests itself seismologically via spatial variations in the relative proportions of phases. This occurs, for example, in the presence of lateral variations in temperature (Anderson 1987). As temperature varies at constant depth, the relative proportions of phases and their compositions vary. Because phases have very different velocities, lateral variations in the velocity of the aggregate occur. The contributions to the temperature derivative of the velocity may, therefore, be separated into an isomorphic part and a metamorphic part, with the former accounting for the influence of temperature on the velocity of individual phases at constant composition and the latter accounting for changes in phase proportions:

$$\left(\frac{\partial \ln X}{\partial T}\right)_P = \left(\frac{\partial \ln X}{\partial T}\right)_{P,\vec{n}} + \left(\frac{\partial \ln X}{\partial \vec{n}}\right)_{P,T} \left(\frac{\partial \vec{n}}{\partial T}\right)_P, \quad (2)$$

where X is a property of the aggregate such as density or velocity, T is temperature, P is pressure, and $\vec{n}$ is the vector specifying the amounts of all end-member species of all phases (Stixrude & Lithgow-Bertelloni 2007). The first term on the right-hand side is the isomorphic part: The derivative is taken at constant amounts and compositions of all coexisting phases. The second term is the metamorphic part and accounts for the variations in phase proportions (and compositions) with temperature.

The metamorphic contribution to seismic heterogeneity is significant, particularly in the upper mantle and in the deep mantle (**Figure 3**). The metamorphic contribution is 50% of the isomorphic contribution in the transition zone and also in the vicinity of the postperovskite-forming reaction near the core-mantle boundary. Tomographic models have limited depth resolution that is comparable in width to the thickness of the transition zone (Ritsema et al. 2007). Nevertheless, some recent tomographic models show variations in amplitude with depth that appear to capture the metamorphic contribution (Megnin & Romanowicz 2000, Ritsema et al. 2004).

If the temperature is sufficiently high, one of the coexisting phases is a melt. The presence of partial melt has a number of important consequences. Mean-field bounding schemes are no longer useful as the Reuss bound on the shear modulus vanishes. The velocity of a partial melt depends on the details of the arrangement of the melt, the melt fraction, and the direction of propagation and polarization of the wave. Considerations of equilibrium-melt microstructure indicate that 0.1% partial melt may lower the shear-wave velocity by as much as 1% (Hammond & Humphreys 2000, Hier-Majumder & Courtier 2011). Because of its buoyancy and mobility, the melt moves with respect to the other phases and coalesces. The process of melt extraction to form crust is very efficient, so that as little as 0.1% partial melt is difficult to retain in the mantle for geologic periods of time (Hirschmann 2010, Stolper et al. 1981). The process of melt migration may therefore be viewed as one that allows heterogeneity to accumulate, magnifying the length scale of heterogeneity from the grain scale to the lithologic scale.

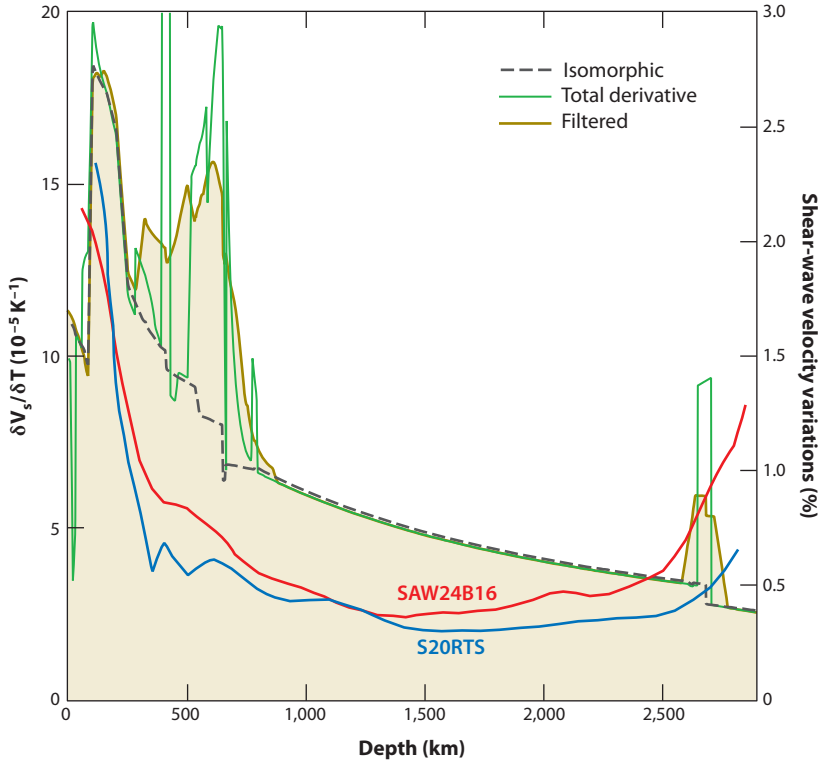

Figure 3

Temperature derivative of the shear-wave velocity computed for pyrolite: the total derivative (*green line*), the isomorphic contribution (*thick dashed gray line*), and the total derivative smoothed with a 200-km box filter (*bold dark yellow line*) to mimic the radial resolution of tomographic models, compared with the amplitude of tomographic models SAW24B16 (Megnin & Romanowicz 2000) and S20RTS (Ritsema et al. 2004).

Lithologic Scale

The nature of lithologic heterogeneity within Earth's mantle is much less well understood than that at smaller scales. The fundamental reason for this is that, whereas grain-scale heterogeneity is largely a product of equilibrium thermodynamics, lithologic heterogeneity is maintained by disequilibrium. Its production and survival depend on mass transport, i.e., timescale and history. For example, the formation of oceanic crust depends not only on the thermodynamics of melting, but also on the fluid dynamics of melt extraction and nonequilibrium reaction with surroundings on ascent (Rudge et al. 2011). The survival of subducted heterogeneity depends on the processes of stretching and folding in the convecting mantle, buoyancy of the heterogeneity, and chemical diffusion.

What is the rate of production of heterogeneity? The rate at which oceanic crust is subducted into the mantle is $\rho_c h_c S$, where ρ_c and h_c are the density and thickness of the oceanic crust, respectively, and S is the areal subduction rate. The rate at which oceanic crust is produced is well constrained over the Cenozoic and part of the Mesozoic (**Figure 4**). Apparent polar wander paths of continents provide some constraints on minimum (latitudinal) plate tectonic rates for earlier times (Ulrich & van der Voo 1981), although some of the plate motion may be due to true polar wander (Evans 2003, Tsai & Stevenson 2007). Some estimate of pre-Mesozoic values of S may

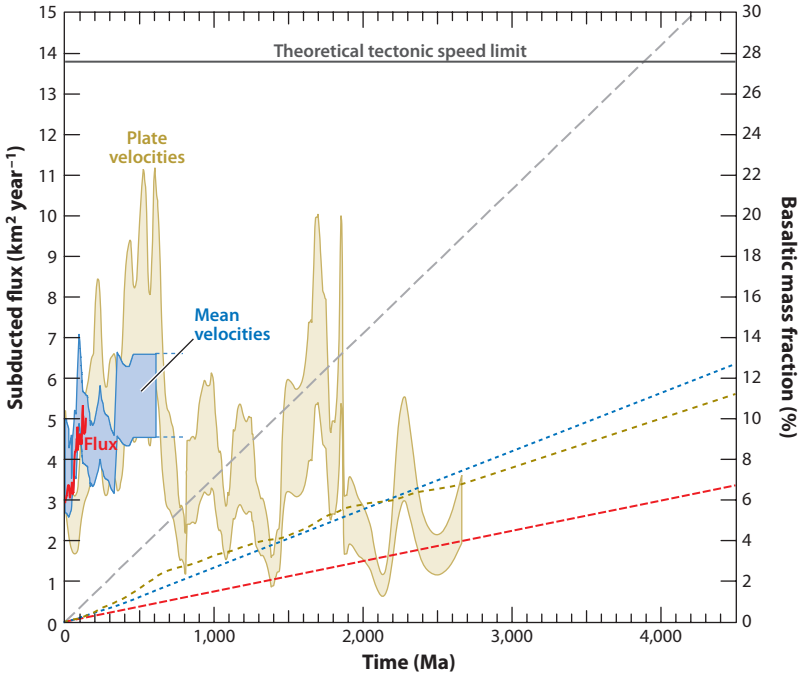

Figure 4

Subducted flux as a function of time (*solid curves and envelopes*, *left-hand axis*) and the time-integrated subducted basalt fraction in the mantle (*dashed curves*, *right-hand axis*) from seafloor ages (*red*) and assuming that the areal rate of seafloor production is equal to the areal rate of subduction (Becker et al. 2009), mean velocities (*blue*) from plate tectonic reconstructions computed by Zhang et al. (2010), latitudinal plate velocities from apparent polar wander paths of four continents (*light brown*) (Ulrich & van der Voo 1981), and a theoretical plate tectonic speed limit (*gray*) (Conrad & Hager 1999). Except for the red line for which measurements of ridge lengths are used, these curves assume a constant length of subduction plate boundaries over time. The upper bound of the blue and light brown envelopes multiplies the velocity by a factor of $(f_S + (1 - f_S)/R_S)^{-1}$, where R_S is the ratio of subducted plate speed to average plate speed. The value of $f_S = 0.38$ is assumed constant; for the blue envelope, the value of R_S varies according to Conrad & Lithgow-Bertelloni (2004) over the Cenozoic and is equal to 2 for earlier times; for the light brown envelope, $R_S = 2$ for all times. Time-integrated subducted basalt fraction is computed assuming a constant crustal thickness of 7 km. The blue and light brown dashed curves are computed assuming the mean value of the corresponding subducted flux envelopes and, for ages beyond those of the data, values equal to that of the oldest datum. The red dashed curve assumes a constant value of the subducted flux equal to that at the present day from the red curve.

be obtained by accounting for the observation that plates attached to subduction zones tend to move more rapidly than those that are not attached by a factor R_S (Conrad & Lithgow-Bertelloni 2004) and assuming the length of subduction zones changed little with time. Integration over the past 4 Ga assuming constant crustal density and thickness yields a mass of subducted oceanic crust 10–15% of the mass of the mantle. In detail, the amount of crust residing in the mantle is slightly less than this because some previously subducted crust is recycled through the plate tectonic system (Allegre & Turcotte 1986).

Estimates of subduction rates may also be obtained from models of Earth's thermal evolution, although these are highly uncertain and give a wide range of values. Conventional thermal evolution models find mantle temperature and plate speeds higher in the past (Davies 2009a),

in agreement with evidence from ancient lavas (Herzberg et al. 2010). But hotter mantle means thicker oceanic crust, which may be more difficult to subduct, leading to slower plate speeds in the past by a factor of two (Korenaga 2008). We note that if the mantle were 200 K hotter in the Archean, crustal thickness would increase to 16 km according to the scaling of Klein & Langmuir (1987), leaving the product Sh approximately constant.

How much of the mantle has been processed through the mid-ocean ridge magmatic system? The rate is $\rho_m h_m S$, where ρ_m is the density of the mantle and h_m is the thickness of the zone of partial melting. A mantle adiabat with a potential temperature of 1600 K intersects the dry peridotite solidus at 60-km depth. In the Archean, h_c and h_m may both be greater by a factor of two, so that it seems reasonable that $h_m/h_c \sim 10$, in which case the amount of mantle processed is 10 times that of the amount of basalt subducted or approximately 100% of the mantle processed through the mid-ocean ridge. This conclusion agrees with a variety of previous analyses (Davies 2009b, Korenaga 2008, Silver et al. 1988).

If we assume that the entire mantle has been processed and that chemical diffusion is negligible, then we can obtain an alternative estimate of the mass of subducted basalt in the mantle, on the basis of the ratio of crust to depleted lithosphere: $\rho_c h_c/\rho_d h_d$, where ρ_d and h_d are the density and thickness, respectively, of the depleted layer. Taking $h_c = 7$ km, $\rho_c = 2{,}900\,\mathrm{kg\,m^{-3}}$, $\rho_d = 3{,}200\,\mathrm{kg\,m^{-3}}$, and $h_d = h_m - h_c = 53$ km, we obtain 12%, similar to the independent estimate above based on subduction rates. Another approach was taken by Xu et al. (2008), who found the fraction of basalt in a mechanical mixture of basalt and harzburgite that yielded a bulk composition identical to pyrolite. The result, 18% basalt, is somewhat greater than the previous estimates. The reason is that Xu et al. (2008) mass-balanced their basalt with the most depleted harzburgite: In reality, the residue of partial melting shows a range of depletions and an average composition less depleted than that of harzburgite.

How long does subducted heterogeneity survive in the mantle? Ultimately, the lifetime of lithologic heterogeneity is limited by the rate of chemical diffusion. This rate can be characterized by the length scale l over which diffusion is operative in time interval τ: $l = \sqrt{D\tau}$, where D is the diffusion coefficient. Chemical diffusion is extremely slow, such that l reaches only 1 m over the age of Earth, assuming a value of D appropriate for magnesium-rich silicate perovskite (**Figure 5**). Thus chemical diffusion operates on length scales much smaller than those of subducted heterogeneity. Indeed, the inefficiency of chemical diffusion is one of the foundations of geochemical studies of provenance (Hofmann & Hart 1978). The rate of chemical diffusion varies little across most of the lower mantle, but may be enhanced in the lower thermal boundary layer due to higher temperature and the unique properties of postperovskite (Ammann et al. 2010). The rate of chemical diffusion may be enhanced by the presence of partial melt or fluids, although, even in this case, the length scale is estimated to be no more than $500\sqrt{(\tau/1\,\mathrm{Ga})}$ m (Hofmann & Magaritz 1977). Chemical diffusion may be slowed or stopped by chemical armoring: the formation of a reaction zone at the boundary between two lithologies or out-of-equilibrium phases that tends to prevent further mass transport (Bina 2010).

Stirring in the mantle reduces the thickness of subducted oceanic crust exponentially (**Figure 5**). The rate of thinning is approximately $h = h_0 \exp(-\dot{\varepsilon}\tau)$, where h_0 is the initial thickness and $\dot{\varepsilon}$ is the strain rate (Spence et al. 1988). For typical values of the strain rate, the thickness of the oceanic crust is reduced to the diffusion length scale in approximately 1–10 Ga. This estimate is compatible with previous analyses (Kellogg & Turcotte 1990). It should be noted that the rate of thinning in mantle convection is an active area of research. The rate is profoundly affected by the character of the flow (chaotic versus laminar), by the relative amounts of pure and shear strain, with the former being much more effective at thinning, and by the presence of toroidal motion (Ferrachat & Ricard 1998, Hoffman & Mckenzie 1985, van Keken & Zhong 1999). The

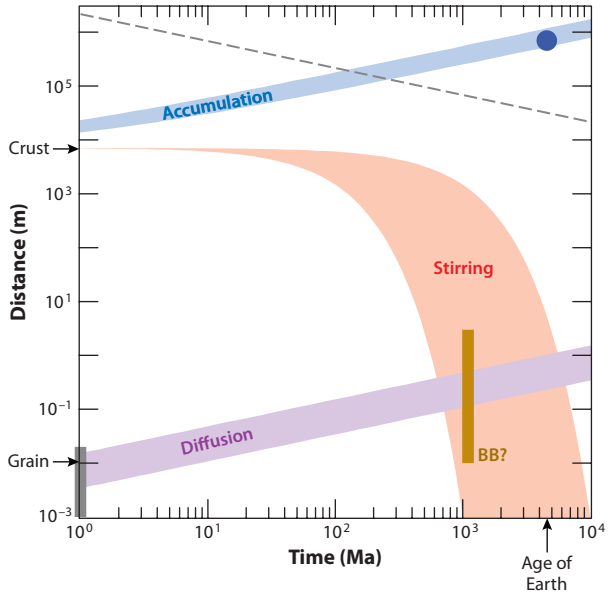

Figure 5

Evolution of length scales relevant to the survival of heterogeneity in the mantle. (*Red*) Flow-induced thinning of heterogeneity with initial thickness equal to that of present day oceanic crust (7 km) assuming exponential thinning (see text) and values of the strain rate ranging from $\dot{\varepsilon} = u/L = 6 \times 10^{-16}\,\mathrm{s}^{-1}$ to one-tenth this value to account for the possible effects of pure versus shear strain partitioning and more sluggish convection in the lower mantle, where u is present-day average plate speed (5.5 cm year^{-1}) and L is the depth of the mantle (2891 km). (*Purple*) Length scales over which chemical diffusion is operative with values of the effective diffusion coefficient appropriate to the lower mantle (0.4–7 $\times$ 10^{-18} m^2 s^{-1}). The width of the envelope corresponds to a range in oxygen fugacity of six orders of magnitude (Holzapfel et al. 2005). (*Blue*) The maximum rate of accumulation of a cylindrical pile of basalt with radius $= \sqrt{vh_c t}$, where v = 1–10 cm year^{-1} is the sinking velocity, assuming that it separates from harzburgite efficiently at the core-mantle boundary and is not re-entrained in the overlying flow. The dashed gray line shows the radius of a Stokes blob that will traverse half the mantle depth in time $t\,r = \sqrt{9L\eta/4g\Delta\rho t}$, where $\eta = 5 \times 10^{22}$ Pa s is the lower mantle viscosity (Lithgow-Bertelloni & Richards 1998), and g is gravitational acceleration for a nominal density contrast $\Delta\rho = 100$ kg m^{-3}. The blue circle represents the thickness of the accumulated pile of basalt in the geodynamic model of Nakagawa et al. (2010). The gold band represents the range of thickness of pyroxenite bands measured in the Beni Bousera (BB) peridotite massif (Pearson & Nowell 2004) and the rhenium-osmium age of melt extraction from the Beni Bousera peridotite (Pearson & Nowell 2004).

efficiency of mixing can vary substantially with position and time even in vigorous time-dependent convection (Farnetani & Samuel 2003).

How rapidly does subducted heterogeneity accumulate at the base of the mantle? The length scale of subducted oceanic crust may be increased via buoyant accumulation (**Figure 5**). Augmentation of the length scale of heterogeneity via buoyant accumulation is apparent in the formation of oceanic crust from melt distributed on the grain scale and the assemblage of the continental crust from dispersed centers of magmatism. Each of these processes depends on the association of heterogeneity with buoyancy. In the case of subducted oceanic crust, the material becomes denser than peridotite in the lower mantle. Dynamical models show substantial accumulation at the base of the mantle for a density contrast of 1% (Christensen & Hofmann 1994, Davies 2009b, Nakagawa et al. 2010). Accumulation opposes thinning and may permit subducted oceanic crust to survive for much longer than 1 Ga in the mantle. Earlier studies envisioned subducted

crust separating on the way down as it encountered the lower mantle (Irifune & Ringwood 1993). However, geodynamical models and measurements of rheology show that delamination cannot occur on such a rapid timescale in the transition zone (Jin et al. 2001, van Keken et al. 1996). Instead, basalt separates from peridotite at the base of the mantle where the viscosity is likely to be substantially reduced because of the basalt thermal boundary layer (Christensen & Hofmann 1994). The unusually soft rheology of the postperovskite phase (Ammann et al. 2010) may assist in the separation of basalt from eclogite in the lowermost mantle. Some of the segregated basalt is re-entrained into the transition zone where it accumulates, although to a lesser extent than at the base of the mantle. The dynamical stability of chemically dense piles at the base of the mantle and their possible connection with hotspots and superswells has been investigated computationally and experimentally (Davaille 1999, McNamara & Zhong 2005).

MINERAL PHYSICS

Scaling Relations

The behavior of materials shows universal patterns and trends that can be used to make general statements about the origins of geophysically observed heterogeneity. Bullen (1963) and Birch (1952) recognized the relationship between measured radial profiles of seismic wave velocities and, respectively, the radial gradient in the density and the pressure derivative of the bulk modulus K'. The Bullen inhomogeneity parameter η is unity if the mantle is homogeneous in bulk composition (lithology), phase, and potential temperature (or entropy) apart from possible small contributions from bulk attenuation (Heinz & Jeanloz 1983). The value of η in the transition zone deviates substantially from unity, consistent to first order with expectations based on experimental mineral physics that this part of the mantle is characterized by a series of phase transformations. But it is not currently known whether the series of expected phase transitions is sufficient to explain radial inhomogeneity in the transition zone or whether radial gradients in bulk composition or entropy may also be required. One problem is that the radial gradient in density in the mantle is not known very precisely. Thus, inhomogeneity, either in bulk composition, entropy, phase, or all three, is permitted throughout within present uncertainties in η. For example, in the middle of the lower mantle, various seismic models fit to the same free oscillation data set find values of η that differ by ~10% (Masters 1979). The most common Earth model, PREM, simply assumes that η is unity in the bulk of the lower mantle (Dziewonski & Anderson 1981).

Temperature is insufficient to explain all the lateral heterogeneity seen in seismic tomography. Some limits can be placed on the nature of thermally induced lateral heterogeneity from mineral physics. The ratio of the lateral variations in S-wave to P-wave velocity at depth z:

$$R = \left(\frac{\delta \ln V_S}{\delta \ln V_P} \right)_z . \tag{3}$$

If lateral variations are solely due to temperature, then we may write the thermodynamic identity

$$R_T = \left[\frac{(1 - A)(\delta_S - 1)}{\Gamma - 1} + A \right]^{-1} , \tag{4}$$

where the subscript T indicates that variations are due only to temperature, $A = (4/3)V_S^2/V_P^2$, $\delta_S = (\partial \ln K_S/\partial \ln \rho)_P$, and $\Gamma = (\partial \ln G/\partial \ln \rho)_P$. Mineral physics measurements find that δ_S, $\Gamma > 1$, in which case the thermal ratio takes on its largest possible value $R_T \to A^{-1} \approx 2.5$ as $\delta_S \to 1$ (Agnon & Bukowinski 1990, Isaak et al. 1992). This is to be compared with the value

determined seismologically, which reaches values as large as 3.8 (Bolton & Masters 2001, Ritsema & van Heijst 2002, Robertson & Woodhouse 1996).

There are two possible mechanisms for increasing the value of R beyond the maximum value of R_T: lateral heterogeneity in phase or lithology (bulk composition). The perovskite to postperovskite transition is likely to contribute to the large value of R, but only over a limited depth interval. Compared with perovskite, postperovskite is faster in V_S but slower in the bulk sound velocity V_B (Wentzcovitch et al. 2006, Wookey et al. 2005). At the transition, $d\ln V_S/dT$ is enhanced (**Figure 2**) and $d\ln V_B/dT$ is reduced. But the transition occurs only over a narrow depth interval and seems unlikely to explain signatures of anomalous V_S-V_P correlation that extend to 1000 km above the core-mantle boundary. Lateral variation in lithology is the most likely explanation for most of the seismically observed signal. Trampert et al. (2004) suggested that correlated variations in temperature, FeO, and SiO_2 concentrations could produce anticorrelation of lateral variations in bulk- and shear-wave velocity.

Mineralogical Mantle Models

To delve deeper into the origins of seismic heterogeneity or the consequences of heterogeneity for dynamics requires a synthesis of the progress that mineral physics has made over the past few decades in mapping out the sequence of phase transformations, and the physical properties of individual phases and assemblages, expected in Earth's mantle. Phase equilibria are now densely mapped at mantle pressure-temperature conditions to pressures well into the lower mantle and, in a few cases and with greater uncertainty in pressure and temperature calibration, extending even to the base of the mantle (Akaogi et al. 1989, Irifune & Ringwood 1993, Shim 2008). Measurements of physical properties, including seismic-wave velocities, have now been made for the first time at mantle pressure-temperature conditions (Higo et al. 2008) and at the pressure of the base of the mantle (Murakami et al. 2007). Although important uncertainties remain, particularly at the experimental limit of combined high pressure and high temperature, which are technically most challenging, it is now possible to construct an interim synthesis of the existing data and to draw some conclusions about the nature of mantle heterogeneity and its impact on mantle dynamics.

HeFESTo is a synthetic model of mantle mineral physics that has been used to explore mantle dynamics and the origin of mantle structure (Stixrude & Lithgow-Bertelloni 2005, 2011). The model is based on the concept of thermodynamic equilibrium under anisotropic stress, which demands that there be a unique assemblage of phases with a unique set of physical properties at any given point in Earth of known pressure, temperature, and bulk composition. Phase equilibria are determined by minimization of an appropriate free energy, and physical properties are related to derivatives of the free energy with respect to thermodynamic conditions (pressure, temperature, etc.). To make contact with seismic observations, standard textbook thermodynamics must be generalized to conditions of anisotropic stress and strain that a material experiences during the passage of a seismic wave. To make contact with geodynamics and seismology, the thermodynamic formulation encompasses the extreme range of pressure and temperature relevant to the mantle, and it includes that set of major elements that play a dominant role in determining phase stability and dynamically relevant properties. The construction of HeFESTo builds on many previous models of mantle thermodynamics, including (*a*) those primarily focused on the computation of phase equilibria but lacking the ability to self-consistently compute seismic-wave velocities (Ganguly et al. 2009, Ricard et al. 2005, Stixrude & Bukowinski 1993); (*b*) those primarily focused on physical properties but without encompassing self-consistent computation of phase equilibria (Duffy & Anderson 1989, Weidner 1985); and (*c*) hybrid models, which assemble information on

physical properties and phase equilibria without computing each self-consistently (Cammarano et al. 2005, Hacker et al. 2003, Ita & Stixrude 1992).

HeFESTo has proved to be a useful tool for investigating the seismically observable consequences of mantle heterogeneity. If pervasive lithologic heterogeneity exists in the mantle, it should be discernible via a combination of seismological observation and mineral physics modeling. The seismic-wave velocities of enriched and depleted material thus provide a link between the geochemical consequences of depletion and geophysical observations. This opens up the possibility to map out the three-dimensional geometry of mantle reservoirs.

GEOPHYSICAL SIGNATURES OF CHEMICAL HETEROGENEITY

Subwavelength Signatures

Chemical heterogeneity may alter the seismic-wave velocity even when the length scale of the heterogeneity is substantially less than the seismic wave. Separating an initially homogeneous rock into two distinct lithologies while maintaining the same bulk chemical composition alters the seismic velocity of the aggregate (Xu et al. 2008). The reason is that the phase assemblage of a lithologically heterogeneous mantle differs from that of pyrolite (**Figure 6**). Schematically, the change in phase assemblage in the upper mantle may be represented by the reaction

$$\mathrm{MgSiO_3(pyrolite) = Mg_2SiO_4(harzburgite) + SiO_2(basalt).} \quad (5)$$

The stabilization of free silica in subducted basalt and the increased proportion of olivine in harzburgite cause the velocity of heterogeneous mantle to exceed that of pyrolite in the transition zone (**Figure 6**). The heterogeneous mantle agrees with seismological models of the absolute velocity in the transition zone, whereas undepleted mantle is too slow (Xu et al. 2008). The better agreement suggests that the transition zone has at least some component of lithologic heterogeneity.

The absolute velocity in the transition zone represents an important test of mantle heterogeneity. However, absolute velocity profiles in the transition zone differ significantly among different one-dimensional seismic models. Rather than comparing with seismic models, one may compare mineralogical models directly with seismic data (Cammarano et al. 2005, 2009; Khan et al. 2008). Ritsema et al. (2009) computed synthetic seismograms of SS precursors directly from HeFESTo mantle structures along a variety of isentropic temperature profiles. The results support the idea of pervasive heterogeneity in the transition zone: Models based on pyrolite required implausibly large potential temperatures to satisfy the difference in arrival time between S410S and S660S precursors. By contrast, models based on a transition zone composed of basalt and harzburgite matched the seismic observations with reasonable potential temperatures.

Phase Transitions and Seismic Reflectors

Lithologic heterogeneity also alters the seismic structure near the core-mantle boundary and the signal of the perovskite to postperovskite transition (**Figure 6**). We find that in a heterogeneous mantle the transition is crossed twice along a geotherm that includes a bottom thermal boundary layer. Evidence of double crossing is seen in seismology (Lay et al. 2006, van der Hilst et al. 2007), supporting the heterogeneous model over the pyrolite model for this region. The double crossing originates in the harzburgite component. In pyrolite and basalt, the transition is crossed only once: The greater proportion of FeO in these compositions slightly deepens the transition so that it occurs beyond the mantle pressure regime at the high temperature of the thermal boundary

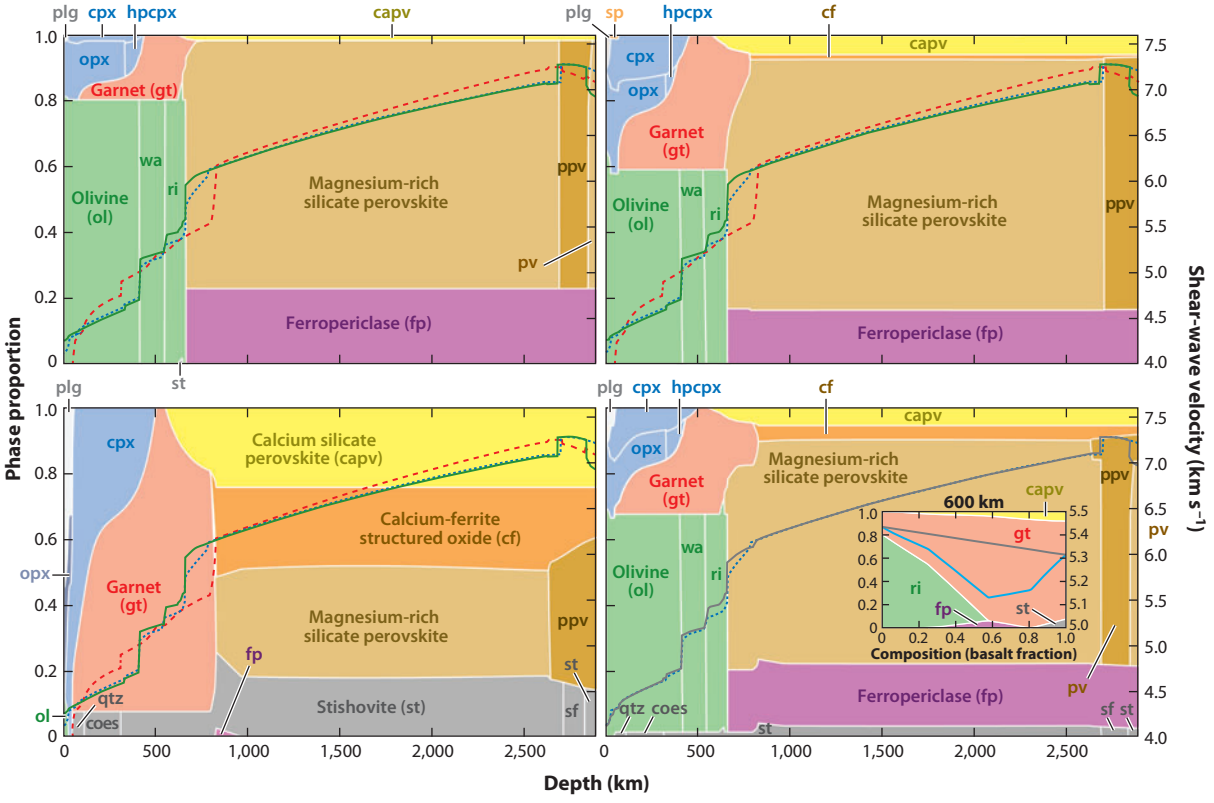

capv = calcium silicate perovskite
cf = calcium-ferrite structured oxide
coes = coesite
cpx = clinopyroxene
fp = ferropericlase
gt = garnet
hpcpx = high-pressure Mg-rich clinopyroxene
ol = olivine
opx = orthopyroxene
plg = plagioclase
ppv = postperovskite
pv = perovskite
qtz = quartz
ri = ringwoodite
sf = seifertite
sp = spinel
st = stishovite
wa = wadsleyite

Shear-wave velocities
Pyrolite
Harzburgite
Basalt
Equilibrium assemblage
Mechanical mixture

Figure 6

Phase proportions (atomic fraction) of (*counterclockwise*, *from top right*) pyrolite, harzburgite, basalt, and a mechanical mixture of 18% basalt and 82% harzburgite equal in overall bulk composition to pyrolite. Superimposed are the shear-wave velocities of pyrolite (*dotted blue line*), harzburgite (*solid green line*), basalt (*dashed red line*), and the mechanical mixture (*solid gray line*). Curves are repeated in multiple panels to permit direct comparison. Inset in the lower right panel shows the origin of the faster velocity in the mechanical mixture. Phase proportions and velocity vary with composition in an equilibrium assemblage (*solid light blue line*) and a mechanical mixture of the end-member compositions (*solid gray line*). Computed with HeFESTo (Stixrude & Lithgow-Bertelloni 2011). All bulk compositions are taken from Xu et al. (2008). Phases are labeled as in **Figure 2**.

layer. It should be noted that the presence or absence of double crossing in the mantle is uncertain at present because the geotherm in the lower thermal boundary layer is poorly constrained and because of conflicting experimental results on the influence of composition on the perovskite to postperovskite transition. For example, Auzende et al. (2008) found that addition of FeO stabilizes postperovskite to lower pressure, in contrast to the study by Hirose et al. (2008) upon which our model is based. By contrast, Catalli et al. (2009) found that addition of FeO substantially broadens

the transition to the point that it may not be able to reflect seismic waves. If solid solution does significantly broaden the transition, harzburgite and a heterogeneous mantle are favored as the origin of deep mantle reflectors because harzburgite is more nearly pure. A heterogeneous deep mantle is also supported by seismic observations of additional reflectors, some of which have been interpreted in terms of the stishovite to seifertite transition that occurs only in highly enriched compositions, such as basalt (Ohta et al. 2008).

Scattering

The seismic-wave velocities of enriched and depleted lithologies differ significantly throughout the mantle (**Figure 7**). The reason is that enrichment alters phase proportions and stabilizes phases that do not exist in depleted compositions. For example, free silica is stable in enriched compositions but not in depleted or undepleted peridotite compositions. Over much of the mantle pressure-temperature regime, free silica is the fastest phase (**Figure 2**), which explains why enriched compositions are faster throughout the lower mantle. At shallow depths (100–300 km), enriched compositions are faster because they contain a higher proportion of garnet (eclogite), which is relatively fast compared with other upper mantle phases. Enriched compositions are not faster everywhere. Garnet is stabilized in enriched compositions to greater depths in the lower mantle, thus deepening the perovskite-forming reaction compared with depleted compositions and slowing enriched compositions in the uppermost lower mantle.

If lithologic heterogeneity is pervasive, the contrast in elastic properties between the two lithologies causes scattering of seismic waves (**Figure 7**). The scattered power depends on the length scale of the lithologic heterogeneity, the velocity contrast between the lithologies, and the frequency of the wave. The contrast in properties between basalt and harzburgite as well as the expected length scales of chemical heterogeneity based on dynamical arguments agree well with studies of seismic scattering from the lower mantle. Hedlin et al. (1997) argued that scattered P-wave energy could be most simply explained by pervasive scatters with length scale 8 km and velocity contrast of 1%, very similar to the properties that we find for enriched lithologic heterogeneity. Similar results for the mantle have been obtained in subsequent studies with larger data sets (Shearer & Earle 2008). Regional studies have found evidence for scattering at length scales of 10–100 km and velocity contrasts of 1–2% (Kaneshima & Helffrich 1998, Kawakatsu & Niu 1994, Vinnik et al. 2001).

GEOCHEMICAL EVIDENCE OF CHEMICAL HETEROGENEITY

Evidence from geochemistry overlaps with that from geophysics in a number of areas in which a picture of the mantle resembling the model shown in **Figure 1*c*** is consistent with geochemical observations. Analyses of mantle-derived lavas show evidence of mantle chemical heterogeneity on length scales ranging from that of the melting process (~100 km in lateral and vertical dimension) to 10,000 km (White 2010). Studies of melt inclusions also show that chemical heterogeneity exists down to the subgrain scale. These results are consistent with a picture of the mantle in which heterogeneity exists on all scales from the chemical diffusion length (~1 cm) to subplanetary scale as in **Figure 1*c***.

There is considerable evidence that some aspects of geochemical diversity can be explained by the presence of subducted crust in the source of mantle-derived lavas. Incompatible element enrichment and strontium, lead, and neodymium isotopic characteristics of ocean island basalt resemble oceanic crust (Hofmann & White 1982). Rhenium-osmium systematics have been interpreted in terms of recycled mafic material in the source of ocean island basalts (Day et al. 2009,

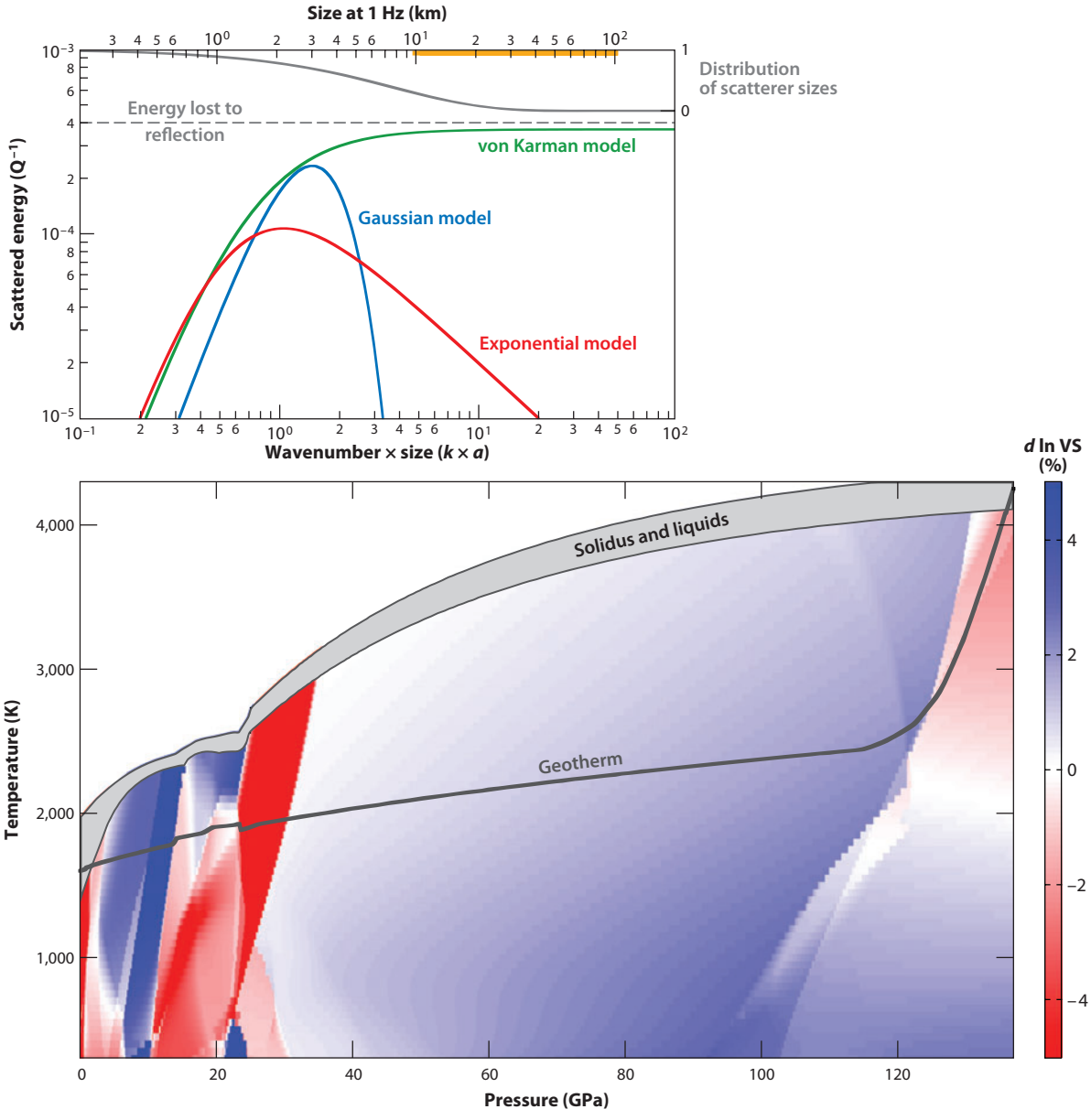

Figure 7

(*Bottom*) Difference in shear-wave velocity between basalt and harzburgite. The geotherm (*thick gray line*) and the solidus and liquidus (*gray envelope*) are from Stixrude et al. (2009). Computed with HeFESTo (Stixrude & Lithgow-Bertelloni 2011). (*Top*) Seismic scattering expressed as the energy lost to scattering per cycle (Q^{-1}) for exponential (*red*), Gaussian (*blue*), and von Karman (*green*) models of randomly distributed heterogeneity with characteristic scale length a according to the theory of Wu (1982) plotted as a function of the dimensionless product of a with the wavenumber of the seismic probe k (*bottom axis*) and in terms of absolute sizes for a 1-Hz P-wave in the lower mantle (*top axis*). Gray horizontal dashed line indicates energy lost to reflection from a plane interface assuming the same velocity contrast (2%) as that of the scattering curves and Birch's law for the density contrast. Solid gray curve (*right-hand axis*) indicates the distribution of scatterer sizes found by Shearer & Earle (2008) to match observations of seismic scattering from the lower mantle. Gold bar indicates the range of length scales of scatterers found by Kaneshima & Helffrich (2010).

Shirey & Walker 1998). The distinctive geochemical signatures of ocean island basalts thus appear to be consistent with the accumulation of some fraction of the subducted basalt at the base of the mantle, the presumptive source of ocean island lavas. Distributed basaltic heterogeneity throughout the mantle is consistent with oxygen isotopic compositions of MORB that are characteristic of interaction with the hydrosphere, indicating the presence of ancient subducted oceanic crust in the MORB source as well (Eiler et al. 2000).

Ocean island and mid-ocean ridge basalts are too enriched in various trace and minor elements to have been formed by partial melting of a homogeneous fertile peridotite (Dasgupta et al. 2010, Hirschmann & Stolper 1996, Prytulak & Elliott 2007, Sobolev et al. 2007). These studies have invoked the presence of 1–10% recycled oceanic crust in the basalt source region to explain the observations.

Xenoliths and ultramafic massifs also point toward a heterogeneous mantle. The compositions of mantle xenoliths and alpine massifs span a wide range that encompasses MORB and depleted peridotite (harzburgite) as well as undepleted peridotitic mantle similar to the classic picture of the MORB source (Hirschmann & Stolper 1996). In some massifs, depleted and enriched material coexist: The Beni Bousera massif in Morocco contains numerous pyroxenite veins within a peridotitic mass (Allegre & Turcotte 1986). These veins have compositions that are similar to MORB and range in thickness from 1 to 300 cm and make up 9% of the rock by volume, consistent with estimates of the amount of enriched material in the mantle derived from lava compositions (Pearson & Nowell 2004). The origin of the pyroxenite veins is currently uncertain, i.e., whether they represent ancient crust that was subducted in the distant past, stirred in the mantle, and returned to the surface largely intact or whether they represent late features of emplacement in the shallow Earth (Bodinier et al. 2008). If we accept the rhenium-osmium model age (Pearson & Nowell 2004) as that of pyroxenite vein formation, we find remarkable consistency between the structure of this massif and expectations based on stirring and chemical diffusion (**Figure 5**).

Can a mantle composed of enriched material and infertile peridotite such as the one depicted in **Figure 1*c*** produce mid-ocean ridge basalt? This is an open question as it has not been considered in detail to our knowledge. Partial melting of a heterogeneous mixture of enriched material and fertile peridotite has been examined (Hirschmann & Stolper 1996, Ito & Mahoney 2005). These studies assume that melting is fractional: Infinitesimal amounts of melt are extracted efficiently and do not react with their surroundings. However, if the peridotite is infertile, the melting process is different: Only the more fusible enriched material produces partial melt on its own. Then, this material must react with the infertile peridotite to produce a MORB-like pooled crustal composition. The chemistry of the product depends on the composition of the partial melt of the enriched material (i.e., the degree and depth of melting) and the extent (rate) of reaction of the partial melt with the infertile peridotite. As an illustration of some of the issues to be considered, Davies (2009b) envisioned some of the partial melts of the basalt fraction refreezing on ascent and being re-entrained in the convecting system. In this context, the infertile peridotite (harzburgite) that we have depicted is an oversimplification. The material residual to MORB is not homogeneous, but it represents a range of depletion with infertile peridotite as one end-member. This range in peridotite compositions and the possibility of reaction between enriched melt with infertile peridotite may help to account for the range of peridotite and pyroxenite xenolith compositions that are observed (Hirschmann & Stolper 1996).

It has long been recognized that CI chondritic meteorites, the presumptive building blocks of Earth, have a higher silicon to magnesium ratio than does the upper mantle (Macdonald & Knopoff 1958). To account for this difference, various authors have advocated the presence of the missing silicon in the core (Ringwood 1961) or the lower mantle (Hart & Zindler 1986). Basalt accumulation in the deep mantle enriches the lower mantle and increases the silicon to

magnesium ratio of the bulk Earth as compared with that of the upper mantle. The amount of basalt enrichment in the lower mantle is uncertain because of additional uncertainties in the total amount of basalt subducted (**Figure 4**), the processing rate of the mantle, and the density contrast between basalt and harzburgite to which dynamical models showing deep basalt accumulation are sensitive (Nakagawa et al. 2010).

FUTURE OUTLOOK

An understanding of material properties and their variations with chemistry, phase, and temperature provides a means for exploring the geophysically observable consequences of chemical heterogeneity. Mineral physics can help to explain features of existing seismological models that indicate nonthermal heterogeneity and can suggest avenues for new seismic observations focused on better constraining chemical heterogeneity. Mineral physics can also help to overcome the difficulties of geophysical detection of chemical heterogeneity: Mineralogical models show that subwavelength lithologic heterogeneity should be detectable, via its influence on aggregate seismic properties, and that thermal, phase, and chemical origins of heterogeneity each have distinctive signatures that allow them to be disentangled.

Mineral physics allows us to relate the geophysical picture of chemical heterogeneity to that derived from other sources of observation including those deriving from volcanism. By tying seismic observations to chemical composition, mineral physics can help to construct a picture of the geometry of chemical heterogeneity that is otherwise difficult to constrain. At first sight, it may appear difficult to reconcile geochemical and geophysical observations because their sensitivities to chemical heterogeneity are so different: Geochemical reservoirs are identified most powerfully in terms of isotopic variations to which seismic-wave propagation is completely insensitive, and seismology is most sensitive to major element chemistry, which is more difficult to analyze in terms of provenance. Yet, making connections between geophysical and geochemical observations is important because it is impossible to determine the size, shape, or location of geochemical reservoirs on the basis of mantle-derived lavas alone. As a result, the literature has provided a number of alternative models, which are difficult to distinguish on the basis of geochemical evidence alone (Tackley 2000). Attempts to correlate trace element and major element variations among ocean island basalts suggest that it may be possible to identify the major element composition of other geochemical reservoirs as well (Jackson & Dasgupta 2008), providing a link between isotope composition and geophysical observables.

The future will also see continued rapid progress on the determination of phase equilibria and physical properties of mantle materials that allow us to detect chemical heterogeneity in geophysical observations. The first measurement of seismic-wave velocities at mantle pressure-temperature conditions was made only recently (Higo et al. 2008), and technical advances promise much tighter constraints on the influence of phase, temperature, and composition on seismic-wave velocities in the deep Earth (Murakami et al. 2009). The study of lower-mantle phase equilibria is still in its infancy, and important steps are already being made to address issues of pressure and temperature calibration and chemical equilibrium (Shim 2008). Ab initio prediction of high-pressure material behavior continues to mature as a complement to experiments. Limitations in terms of accuracy and the structural complexity, length, and timescales of simulations are being overcome with novel methodologies and increased computer power (Ammann et al. 2010, Driver et al. 2010, Stackhouse et al. 2010, Wu & Wentzcovitch 2011). These experimental and theoretical advances, combined with continued expansion of the seismic data set via initiatives such as USArray, promise major progress on our understanding of mantle chemical heterogeneity in the near future.

DISCLOSURE STATEMENT

The authors are not aware of any affiliations, memberships, funding, or financial holdings that might be perceived as affecting the objectivity of this review.

ACKNOWLEDGMENTS

This research was supported by the U.S. National Science Foundation under award EAR-0079980 and by the National Environmental Research Council (UK) under award NE/H007636/1. We thank J.P. Brodholt, B. Buffett, C.P. Conrad, and R. van der Voo for helpful discussions.

LITERATURE CITED

Agnon A, Bukowinski MST. 1990. δ_S at high pressure and dlnVs/dlnVp in the lower mantle. *Geophys. Res. Lett.* 17:1149–52

Akaogi M, Ito E, Navrotsky A. 1989. Olivine-modified spinel-spinel transitions in the system Mg_2SiO_4-Fe_2SiO_4: calorimetric measurements, thermochemical calculation, and geophysical application. *J. Geophys. Res.* 94:15671–85

Allegre CJ, Turcotte DL. 1986. Implications of a two-component marble-cake mantle. *Nature* 323:123–27

Ammann MW, Brodholt JP, Wookey J, Dobson DP. 2010. First-principles constraints on diffusion in lower-mantle minerals and a weak D″ layer. *Nature* 465:462–65

Anderson DL. 1987. Thermally induced phase-changes, lateral heterogeneity of the mantle, continental roots, and deep slab anomalies. *J. Geophys. Res.* 92:13968–80

Auzende AL, Badro J, Ryerson FJ, Weber PK, Fallon SJ, et al. 2008. Element partitioning between magnesium silicate perovskite and ferropericlase: new insights into bulk lower-mantle geochemistry. *Earth Planet. Sci. Lett.* 269:164–74

Backus GE. 1962. Long-wave elastic anisotropy produced by horizontal layering. *J. Geophys. Res.* 67:4427–40

Becker TW, Conrad CP, Buffett B, Muller RD. 2009. Past and present seafloor age distributions and the temporal evolution of plate tectonic heat transport. *Earth Planet. Sci. Lett.* 278:233–42

Bina CR. 2010. Scale limits of free-silica seismic scatterers in the lower mantle. *Phys. Earth Planet. Inter.* 183:110–14

Birch F. 1952. Elasticity and constitution of the Earth's interior. *J. Geophys. Res.* 57:227–86

Bodinier JL, Garrido CJ, Chanefo I, Bruguier O, Gervilla F. 2008. Origin of pyroxenite-peridotite veined mantle by refertilization reactions: evidence from the Ronda peridotite (Southern Spain). *J. Petrol.* 49:999–1025

Bolton H, Masters G. 2001. Travel times of *P* and *S* from the global digital seismic networks: implications for the relative variation of *P* and *S* velocity in the mantle. *J. Geophys. Res.* 106:13527–40

Born M, Huang K. 1954. *Dynamical Theory of Crystal Lattices*. Oxford: Clarendon

Boyet M, Carlson RW. 2005. ^{142}Nd evidence for early (>4.53 Ga) global differentiation of the silicate Earth. *Science* 309:576–81

Brandon AD, Walker RJ. 2005. The debate over core-mantle interaction. *Earth Planet. Sci. Lett.* 232:211–25

Bukowinski MST. 1994. Quantum geophysics. *Annu. Rev. Earth Planet. Sci.* 22:167–205

Bullen KE. 1963. An index of degree of chemical inhomogeneity in the Earth. *Geophys. J. Int.* 7:584–92

Cammarano F, Goes S, Deuss A, Giardini D. 2005. Is a pyrolitic adiabatic mantle compatible with seismic data? *Earth Planet. Sci. Lett.* 232:227–43

Cammarano, F, Romanowicz B, Stixrude L, Lithgow-Bertelloni C, Xu W. 2009. Inferring the thermochemical structure of the upper mantle from seismic data. *Geophys. J. Int.* 179:1169–85

Catalli K, Shim SH, Prakapenka V. 2009. Thickness and Clapeyron slope of the post-perovskite boundary. *Nature* 462:782–86

Chen CW, Rondenay S, Evans RL, Snyder DB. 2009. Geophysical detection of relict metasomatism from an Archean (similar to 3.5 Ga) subduction zone. *Science* 326:1089–91
Christensen UR, Hofmann AW. 1994. Segregation of subducted oceanic-crust in the convecting mantle. *J. Geophys. Res.* 99:19867–84
Conrad CP, Hager BH. 1999. The thermal evolution of an Earth with strong subduction zones. *Geophys. Res. Lett.* 26:3041–44
Conrad CP, Lithgow-Bertelloni C. 2004. The temporal evolution of plate-driving forces: importance of "slab suction" versus "slab pull" during the Cenozoic. *J. Geophys. Res.* 109:B10407
Dasgupta R, Jackson MG, Lee CTA. 2010. Major element chemistry of ocean island basalts: conditions of mantle melting and heterogeneity of mantle source. *Earth Planet. Sci. Lett.* 289:377–92
Davaille A. 1999. Simultaneous generation of hotspots and superswells by convection in a heterogeneous planetary mantle. *Nature* 402:756–60
Davidson JP, Morgan DJ, Charlier BLA, Harlou R, Hora JM. 2007. Microsampling and isotopic analysis of igneous rocks: implications for the study of magmatic systems. *Annu. Rev. Earth Planet. Sci.* 35:273–311
Davies GF. 1984. Geophysical and isotopic constraints on mantle convection: an interim synthesis. *J. Geophys. Res.* 89:6017–40
Davies GF. 2009a. Effect of plate bending on the Urey ratio and the thermal evolution of the mantle. *Earth Planet. Sci. Lett.* 287:513–18
Davies GF. 2009b. Reconciling the geophysical and geochemical mantles: plume flows, heterogeneities, and disequilibrium. *Geochem. Geophys. Geosyst.* 10:Q10008
Day JMD, Pearson DG, Macpherson CG, Lowry D, Carracedo JC. 2009. Pyroxenite-rich mantle formed by recycled oceanic lithosphere: oxygen-osmium isotope evidence from Canary Island lavas. *Geology* 37:555–58
Driver KP, Cohen RE, Wu ZG, Militzer B, Rios PL, et al. 2010. Quantum Monte Carlo computations of phase stability, equations of state, and elasticity of high-pressure silica. *Proc. Natl. Acad. Sci. USA* 107:9519–24
Duffy TS, Anderson DL. 1989. Seismic velocities in mantle minerals and the mineralogy of the upper mantle. *J. Geophys. Res.* 94:1895–912
Dziewonski AM, Anderson DL. 1981. Preliminary reference Earth model. *Phys. Earth Planet. Inter.* 25:297–356
Eiler JM, Schiano P, Kitchen N, Stolper EM. 2000. Oxygen-isotope evidence for recycled crust in the sources of mid-ocean-ridge basalts. *Nature* 403:530–34
Evans DAD. 2003. True polar wander and supercontinents. *Tectonophysics* 362:303–20
Farnetani CG, Samuel H. 2003. Lagrangian structures and stirring in the Earth's mantle. *Earth Planet. Sci. Lett.* 206:335–48
Fei YW, Wang YB. 2000. High-pressure and high-temperature powder diffraction. *High Temp. High Press. Cryst. Chem.* 41:521–57
Ferrachat S, Ricard Y. 1998. Regular vs. chaotic mantle mixing. *Earth Planet. Sci. Lett.* 155:75–86
Fukao Y, Obayashi M, Nakakuki T, Deep Slab Project Group. 2009. Stagnant slab: a review. *Annu. Rev. Earth Planet. Sci.* 37:19–46
Ganguly J. 2001. Thermodynamic modeling of solid solutions. In *Solid Solutions in Silicate and Oxide Systems*, ed. CA Geiger, pp. 37–70. Budapest: Eötvös Univ. Press
Ganguly J, Freed AM, Saxena SK. 2009. Density profiles of oceanic slabs and surrounding mantle: integrated thermodynamic and thermal modeling, and implications for the fate of slabs at the 660 km discontinuity. *Phys. Earth Planet. Inter.* 172:257–67
Grand SP, van der Hilst RD, Widiyantoro S. 1997. Global seismic tomography: a snapshot of convection in the Earth. *GSA Today* 7:1–7
Green DH, Ringwood AE. 1967. The genesis of basaltic magmas. *Contrib. Mineral. Petrol.* 15:103–90
Hacker BR, Abers GA, Peacock SM. 2003. Subduction factory: 1. Theoretical mineralogy, densities, seismic wave speeds, and H_2O contents. *J. Geophys. Res.* 108:2029
Hammond WC, Humphreys ED. 2000. Upper mantle seismic wave velocity: effects of realistic partial melt geometries. *J. Geophys. Res.* 105:10975–86
Hart SR, Zindler A. 1986. In search of a bulk-Earth composition. *Chem. Geol.* 57:247–67
Hashin Z, Shtrikman S. 1963. A variational approach to the theory of the elastic behaviour of multiphase materials. *J. Mech. Phys. Solids* 11:127–40

Hedlin MAH, Shearer PM, Earle PS. 1997. Seismic evidence for small-scale heterogeneity throughout the Earth's mantle. *Nature* 387:145–50
Heinz DL, Jeanloz R. 1983. Inhomogeneity parameter of a homogeneous Earth. *Nature* 301:138–39
Helffrich GR, Wood BJ. 2001. The Earth's mantle. *Nature* 412:501–7
Herzberg C, Condie K, Korenaga J. 2010. Thermal history of the Earth and its petrological expression. *Earth Planet. Sci. Lett.* 292:79–88
Hier-Majumder S, Courtier A. 2011. Seismic signature of small melt fraction atop the transition zone. *Earth Planet. Sci. Lett.* 308:334–42
Higo Y, Inoue T, Irifune T, Funakoshi KI, Li BS. 2008. Elastic wave velocities of $(Mg_{0.91}Fe_{0.09})_2SiO_4$ ringwoodite under *P-T* conditions of the mantle transition region. *Phys. Earth Planet. Inter.* 166:167–74
Hiraga T, Anderson IM, Kohlstedt DL. 2004. Grain boundaries as reservoirs of incompatible elements in the Earth's mantle. *Nature* 427:699–703
Hirose K, Takafuji N, Fujino K, Shieh SR, Duffy TS. 2008. Iron partitioning between perovskite and post-perovskite: a transmission electron microscope study. *Am. Mineral.* 93:1678–81
Hirschmann MM. 2010. Partial melt in the oceanic low velocity zone. *Phys. Earth Planet. Inter.* 179:60–71
Hirschmann MM, Stolper EM. 1996. A possible role for garnet pyroxenite in the origin of the "garnet signature" in MORB. *Contrib. Mineral. Petrol.* 124:185–208
Hoffman NRA, Mckenzie DP. 1985. The destruction of geochemical heterogeneities by differential fluid motions during mantle convection. *Geophys. J. R. Astron. Soc.* 82:163–206
Hofmann AW, Hart SR. 1978. Assessment of local and regional isotopic equilibrium in mantle. *Earth Planet. Sci. Lett.* 38:44–62
Hofmann AW, Magaritz M. 1977. Diffusion of Ca, Sr, Ba, and Co in a basalt melt: implications for geochemistry of mantle. *J. Geophys. Res.* 82:5432–40
Hofmann AW, White WM. 1982. Mantle plumes from ancient oceanic-crust. *Earth Planet. Sci. Lett.* 57:421–36
Holzapfel C, Rubie DC, Frost DJ, Langenhorst F. 2005. Fe-Mg interdiffusion in $(Mg,Fe)SiO_3$ perovskite and lower mantle reequilibration. *Science* 309:1707–10
Irifune T, Ringwood AE. 1993. Phase transformations in subducted oceanic crust and buoyancy relationships at depths of 600–800 km in the mantle. *Earth Planet. Sci. Lett.* 117:101–10
Isaak DG, Anderson OL, Cohen RE. 1992. The relationship between shear and compressional velocities at high pressures: reconciliation of seismic tomography and mineral physics. *Geophys. Res. Lett.* 19:741–44
Ita J, Stixrude L. 1992. Petrology, elasticity, and composition of the mantle transition zone. *J. Geophys. Res.* 97:6849–66
Ito G, Mahoney JJ. 2005. Flow and melting of a heterogeneous mantle: 1. Method and importance to the geochemistry of ocean island and mid-ocean ridge basalts. *Earth Planet. Sci. Lett.* 230:29–46
Jackson MG, Dasgupta R. 2008. Compositions of HIMU, EM1, and EM2 from global trends between radiogenic isotopes and major elements in ocean island basalts. *Earth Planet. Sci. Lett.* 276:175–86
Jeanloz R, Morris S. 1986. Temperature distribution in the crust and mantle. *Annu. Rev. Earth Planet. Sci.* 14:377–415
Jin ZM, Zhang J, Green HW, Jin S. 2001. Eclogite rheology: implications for subducted lithosphere. *Geology* 29:667–70
Kaneshima S, Helffrich G. 1998. Detection of lower mantle scatterers northeast of the Marianna subduction zone using short-period array data. *J. Geophys. Res.* 103:4825–38
Kaneshima S, Helffrich G. 2010. Small-scale heterogeneity in the mid-lower mantle beneath the circum-Pacific area. *Phys. Earth Planet. Inter.* 183:91–103
Karki BB, Stixrude L, Wentzcovitch RM. 2001. High-pressure elastic properties of major materials of Earth's mantle from first principles. *Rev. Geophys.* 39:507–34
Kawakatsu H, Niu FL. 1994. Seismic evidence for a 920-km discontinuity in the mantle. *Nature* 371:301–5
Kellogg LH, Turcotte DL. 1990. Mixing and the distribution of heterogeneities in a chaotically convecting mantle. *J. Geophys. Res.* 95:421–32
Khan A, Connolly JAD, Taylor SR. 2008. Inversion of seismic and geodetic data for the major element chemistry and temperature of the Earth's mantle. *J. Geophys. Res.* 113:B09308

Klein EM, Langmuir CH. 1987. Global correlations of ocean ridge basalt chemistry with axial depth and crustal thickness. *J. Geophys. Res.* 92:8089–115
Knittle E, Jeanloz R. 1991. Earth's core-mantle boundary: results of experiments at high pressures and temperatures. *Science* 251:1438–43
Kohn W. 1999. Nobel lecture: electronic structure of matter—wave functions and density functionals. *Rev. Mod. Phys.* 71:1253–66
Kohn W, Sham LJ. 1965. Self-consistent equations including exchange and correlation effects. *Phys. Rev.* 140:A1133–38
Korenaga J. 2008. Plate tectonics, flood basalts and the evolution of Earth's oceans. *Terra Nova* 20:419–39
Labrosse S, Hernlund JW, Coltice N. 2007. A crystallizing dense magma ocean at the base of the Earth's mantle. *Nature* 450:866–69
Lay T, Hernlund J, Garnero EJ, Thorne MS. 2006. A post-perovskite lens and D″ heat flux beneath the central Pacific. *Science* 314:1272–76
Lee CTA, Luffi P, Hoink T, Li J, Dasgupta R, Hernlund J. 2010. Upside-down differentiation and generation of a 'primordial' lower mantle. *Nature* 463:930–35
Lithgow-Bertelloni C, Richards MA. 1998. The dynamics of Cenozoic and Mesozoic plate motions. *Rev. Geophys.* 36:27–78
Loubet M, Sassi R, Didonato G. 1988. Mantle heterogeneities: a combined isotope and trace element approach and evidence for recycled continental crust materials in some OIB sources. *Earth Planet. Sci. Lett.* 89:299–315
Macdonald GJF, Knopoff L. 1958. On the chemical composition of the outer core. *Geophys. J. R. Astron. Soc.* 1:284–97
Masters TG. 1979. Observational constraints on the chemical and thermal structure of the Earth's deep interior. *Geophys. J. R. Astron. Soc.* 57:507–34
Matas J, Bass J, Ricard Y, Mattern E, Bukowinski MSI. 2007. On the bulk composition of the lower mantle: predictions and limitations from generalized inversion of radial seismic profiles. *Geophys. J. Int.* 170:764–80
McKenzie D, Bickle MJ. 1988. The volume and composition of melt generated by extension of the lithosphere. *J. Petrol.* 29:625–79
McNamara AK, Zhong SJ. 2005. Thermochemical structures beneath Africa and the Pacific Ocean. *Nature* 437:1136–39
Megnin C, Romanowicz B. 2000. The three-dimensional shear velocity structure of the mantle from the inversion of body, surface and higher-mode waveforms. *Geophys. J. Int.* 143:709–28
Murakami M, Asahara Y, Ohishi Y, Hirao N, Hirose K. 2009. Development of in situ Brillouin spectroscopy at high pressure and high temperature with synchrotron radiation and infrared laser heating system: application to the Earth's deep interior. *Phys. Earth Planet. Inter.* 174:282–91
Murakami M, Sinogeikin SV, Hellwig H, Bass JD, Li J. 2007. Sound velocity of $MgSiO_3$ perovskite to Mbar pressure. *Earth Planet. Sci. Lett.* 256:47–54
Nakagawa T, Tackley PJ, Deschamps F, Connolly JAD. 2010. The influence of MORB and harzburgite composition on thermo-chemical mantle convection in a 3-D spherical shell with self-consistently calculated mineral physics. *Earth Planet. Sci. Lett.* 296:403–12
Ni SD, Tan E, Gurnis M, Helmberger D. 2002. Sharp sides to the African superplume. *Science* 296:1850–52
Nimmo F, Price GD, Brodholt J, Gubbins D. 2004. The influence of potassium on core and geodynamo evolution. *Geophys. J. Int.* 156:363–76
Nutman AP. 2006. Antiquity of the oceans and continents. *Elements* 2:223–27
Oganov AR, Brodholt JP, Price GD. 2002. Ab initio theory of phase transitions and thermoelasticity of minerals. In *Energy Modelling in Minerals*, ed. CM Gramaccioli, pp. 83–170. Budapest: Eötvös Univ. Press
Ohta K, Hirose K, Lay T, Sata N, Ohishi Y. 2008. Phase transitions in pyrolite and MORB at lowermost mantle conditions: implications for a MORB-rich pile above the core-mantle boundary. *Earth Planet. Sci. Lett.* 267:107–17
Parsons B. 1982. Causes and consequences of the relation between area and age of the ocean floor. *J. Geophys. Res.* 87:289–302

Pearson DG, Nowell GM. 2004. Re-Os and Lu-Hf isotope constraints on the origin and age of pyroxenites from the Beni Bousera peridotite massif: implications for mixed peridotite-pyroxenite mantle sources. *J. Petrol.* 45:439–55

Plank T, Langmuir CH. 1998. The chemical composition of subducting sediment and its consequences for the crust and mantle. *Chem. Geol.* 145:325–94

Prytulak J, Elliott T. 2007. TiO_2 enrichment in ocean island basalts. *Earth Planet. Sci. Lett.* 263:388–403

Reymer A, Schubert G. 1984. Phanerozoic addition rates to the continental crust and crustal growth. *Tectonics* 3:63–77

Ricard Y, Mattern E, Matas J. 2005. Synthetic tomographic images of slabs from mineral physics. In *Earth's Deep Mantle: Structure, Composition, and Evolution*, ed. RD van der Hilst, JD Bass, J Matas, J Trampert, pp. 283–300. Washington, DC: Am. Geophys. Union

Ringwood AE. 1961. Silicon in the metal phase of enstatite chondrites and some geochemical implications. *Geochim. Cosmochim. Acta* 25:1–13

Ritsema J, McNamara AK, Bull AL. 2007. Tomographic filtering of geodynamic models: implications for model interpretation and large-scale mantle structure. *J. Geophys. Res.* 112:B01303

Ritsema J, van Heijst HJ. 2002. Constraints on the correlation of *P*- and *S*-wave velocity heterogeneity in the mantle from *P*, *PP*, *PPP* and *PKP*ab travel times. *Geophys. J. Int.* 149:482–89

Ritsema J, van Heijst HJ, Woodhouse JH. 2004. Global transition zone tomography. *J. Geophys. Res.* 109:B02302

Ritsema J, Xu WB, Stixrude L, Lithgow-Bertelloni C. 2009. Estimates of the transition zone temperature in a mechanically mixed upper mantle. *Earth Planet. Sci. Lett.* 277:244–52

Robertson GS, Woodhouse JH. 1996. Ratio of relative *S* to *P* velocity heterogeneity in the lower mantle. *J. Geophys. Res.* 101:20041–52

Rudge JF, Bercovici D, Spiegelman M. 2011. Disequilibrium melting of a two-phase multicomponent mantle. *Geophys. J. Int.* 184:699–718

Shearer PM, Earle PS. 2008. Observing and modeling elastic scattering in the deep Earth. *Adv. Geophys.* 50:167–93

Shim SH. 2008. The postperovskite transition. *Annu. Rev. Earth Planet. Sci.* 36:569–99

Shirey SB, Richardson SH. 2011. Start of the Wilson cycle at 3 Ga shown by diamonds from subcontinental mantle. *Science* 333:434–36

Shirey SB, Walker RJ. 1998. The Re-Os isotope system in cosmochemistry and high-temperature geochemistry. *Annu. Rev. Earth Planet. Sci.* 26:423–500

Silver PG, Carlson RW, Olson P. 1988. Deep slabs, geochemical heterogeneity, and the large-scale structure of mantle convection: investigation of an enduring paradox. *Annu. Rev. Earth Planet. Sci.* 16:477–541

Sobolev AV, Hofmann AW, Kuzmin DV, Yaxley GM, Arndt NT, et al. 2007. The amount of recycled crust in sources of mantle-derived melts. *Science* 316:412–17

Spackman MA, Hill RJ, Gibbs GV. 1987. Exploration of structure and bonding in stishovite with Fourier and pseudoatom refinement methods using single-crystal and powder X-ray diffraction data. *Phys. Chem. Miner.* 14:139–50

Spence DA, Ockendon JR, Wilmott P, Turcotte DL, Kellogg LH. 1988. Convective mixing in the mantle: the role of viscosity differences. *Geophys. J. Int.* 95:79–86

Stackhouse S, Stixrude L, Karki BB. 2010. Thermal conductivity of periclase (MgO) from first principles. *Phys. Rev. Lett.* 104:208501

Steinle-Neumann G, Stixrude L, Cohen RE. 2002. Physical properties of iron in the inner core. In *Core Structure, Dynamics, and Rotation*, ed. V Dehant, K Creager, S Zatman, S-I Karato, pp. 137–61. Washington, DC: Am. Geophys. Union

Stixrude L, Bukowinski MST. 1993. Thermodynamic analysis of the system MgO-FeO-SiO_2 at high pressure and the structure of the lowermost mantle. In *Evolution of the Earth and Planets*, ed. E Takahashi, R Jeanloz, D Rubie, pp. 131–42. Washington, DC: Int. Union Geodesy Geophys.

Stixrude L, Cohen RE, Hemley RJ. 1998. Theory of minerals at high pressure. *Rev. Mineral.* 37:639–71

Stixrude L, de Koker N, Sun N, Mookherjee M, Karki BB. 2009. Thermodynamics of silicate liquids in the deep Earth. *Earth Planet. Sci. Lett.* 278:226–32

Stixrude L, Hemley RJ, Fei Y, Mao HK. 1992. Thermoelasticity of silicate perovskite and magnesiowüstite and stratification of the Earth's mantle. *Science* 257:1099–101

Stixrude L, Jeanloz R. 2007. Constraints on seismic models from other disciplines: constraints from mineral physics on seismological models. In *Seismology and Structure of the Earth*, ed. AM Dziewonski, B Romanowicz, pp. 775–803. Amsterdam: Elsevier

Stixrude L, Lithgow-Bertelloni C. 2005. Thermodynamics of mantle minerals: I. Physical properties. *Geophys. J. Int.* 162:610–32

Stixrude L, Lithgow-Bertelloni C. 2007. Influence of phase transformations on lateral heterogeneity and dynamics in Earth's mantle. *Earth Planet. Sci. Lett.* 263:45–55

Stixrude L, Lithgow-Bertelloni C. 2011. Thermodynamics of mantle minerals: II. Phase equilibria. *Geophys. J. Int.* 184:1180–213

Stolper E, Walker D, Hager BH, Hays JF. 1981. Melt segregation from partially molten source regions: the importance of melt density and source region size. *J. Geophys. Res.* 86:6261–71

Tackley PJ. 2000. Mantle convection and plate tectonics: toward an integrated physical and chemical theory. *Science* 288:2002–7

Takafuji N, Hirose K, Mitome M, Bando Y. 2005. Solubilities of O and Si in liquid iron in equilibrium with $(Mg,Fe)SiO_3$ perovskite and the light elements in the core. *Geophys. Res. Lett.* 32:L06313

Taylor SR, Mclennan SM. 1995. The geochemical evolution of the continental crust. *Rev. Geophys.* 33:241–65

Trampert J, Deschamps F, Resovsky J, Yuen D. 2004. Probabilistic tomography maps chemical heterogeneities throughout the lower mantle. *Science* 306:853–56

Tsai VC, Stevenson DJ. 2007. Theoretical constraints on true polar wander. *J. Geophys. Res.* 112:B05415

Ulrich L, van der Voo R. 1981. Minimum continental velocities with respect to the pole since the Archean. *Tectonophysics* 74:17–27

van der Hilst RD, de Hoop MV, Wang P, Shim SH, Ma P, Tenorio L. 2007. Seismostratigraphy and thermal structure of Earth's core-mantle boundary region. *Science* 315:1813–17

van der Meer DG, Spakman W, van Hinsbergen DJJ, Amaru ML, Torsvik TH. 2010. Towards absolute plate motions constrained by lower-mantle slab remnants. *Nature Geoscience* 3:36–40

van Keken P, Zhong SJ. 1999. Mixing in a 3D spherical model of present-day mantle convection. *Earth Planet. Sci. Lett.* 171:533–47

van Keken PE, Karato S, Yuen DA. 1996. Rheological control of oceanic crust separation in the transition zone. *Geophys. Res. Lett.* 23:1821–24

Vinnik L, Kato M, Kawakatsu H. 2001. Search for seismic discontinuities in the lower mantle. *Geophys. J. Int.* 147:41–56

Watt JP, Davies GF, Connell RJO. 1976. The elastic properties of composite materials. *Rev. Geophys.* 14:541–63

Weaver BL. 1991. The origin of ocean island basalt end-member compositions: trace-element and isotopic constraints. *Earth Planet. Sci. Lett.* 104:381–97

Weidner DJ. 1985. A mineral physics test of a pyrolite mantle. *Geophys. Res. Lett.* 12:417–20

Wentzcovitch RM, Tsuchiya T, Tsuchiya J. 2006. $MgSiO_3$ postperovskite at D″ conditions. *Proc. Natl. Acad. Sci. USA* 103:543–46

White RS, Mckenzie D, Onions RK. 1992. Oceanic crustal thickness from seismic measurements and rare-Earth element inversions. *J. Geophys. Res.* 97:19683–715

White WM. 2010. Oceanic island basalts and mantle plumes: the geochemical perspective. *Annu. Rev. Earth Planet. Sci.* 38:133–60

Wookey J, Stackhouse S, Kendall JM, Brodholt J, Price GD. 2005. Efficacy of the post-perovskite phase as an explanation for lowermost-mantle seismic properties. *Nature* 438:1004–7

Workman RK, Hart SR. 2005. Major and trace element composition of the depleted MORB mantle (DMM). *Earth Planet. Sci. Lett.* 231:53–72

Wu RS. 1982. Attenuation of short period seismic waves due to scattering. *Geophys. Res. Lett.* 9:9–12

Wu ZQ, Wentzcovitch RM. 2011. Quasiharmonic thermal elasticity of crystals: an analytical approach. *Phys. Rev. B* 83:184115

Xu WB, Lithgow-Bertelloni C, Stixrude L, Ritsema J. 2008. The effect of bulk composition and temperature on mantle seismic structure. *Earth Planet. Sci. Lett.* 275:70–79

Ye K, Cong BL, Ye DI. 2000. The possible subduction of continental material to depths greater than 200 km. *Nature* 407:734–36

Zhang N, Zhong SJ, Leng W, Li ZX. 2010. A model for the evolution of the Earth's mantle structure since the Early Paleozoic. *J. Geophys. Res.* 115:B06401

Annual Review
of Earth and
Planetary Sciences
Volume 40, 2012

Contents

Indexes

Errata

An online log of corrections to *Annual Review of Earth and Planetary Sciences* articles may be found at http://earth.annualreviews.org